

# Theory of the collapsing axisymmetric cavity

J. Eggers<sup>1</sup>, M.A. Fontelos<sup>2</sup>, D. Leppinen<sup>3</sup>, J.H. Snoeijer<sup>1</sup>

*School of Mathematics, University of Bristol, University Walk, Bristol BS8 1TW, UK<sup>1</sup>*

*Departamento de Matemáticas, Consejo Superior de Investigaciones Científicas, C/ Serrano 123, 28006 Madrid, Spain<sup>2</sup>*

*School of Mathematics, University of Birmingham, Edgbaston Birmingham B15 2TT, UK<sup>3</sup>*

(Dated: February 9, 2008)

We investigate the collapse of an axisymmetric cavity or bubble inside a fluid of small viscosity, like water. Any effects of the gas inside the cavity as well as of the fluid viscosity are neglected. Using a slender-body description, we show that the minimum radius of the cavity scales like  $h_0 \propto t'^\alpha$ , where  $t'$  is the time from collapse. The exponent  $\alpha$  very slowly approaches a universal value according to  $\alpha = 1/2 + 1/(4\sqrt{-\ln(t')})$ . Thus, as observed in a number of recent experiments, the scaling can easily be interpreted as evidence of a single non-trivial scaling exponent. Our predictions are confirmed by numerical simulations.

PACS numbers: Valid PACS appear here

Over the last decade, there has been considerable progress in understanding the pinch-off of fluid drops, described by a set of universal scaling exponents, independent of the initial conditions [1, 2]. The driving is provided for by surface tension, the value of the exponents depend on the forces opposing it: inertia, viscosity, or combinations thereof. Bubble collapse appears to be a special case of an inviscid fluid drop breaking up inside another inviscid fluid, which is a well studied problem [3, 4, 5]: the minimum drop radius scales like  $h_0 \propto t'^{2/3}$ , where  $t' = t_0 - t$  and  $t_0$  is the pinch-off time. Thus, huge excitement was caused by the results of recent experiments on the pinch-off of an air bubble [6, 7, 8, 9, 10], or the collapse of a cavity [11] in water, which resulted in a radically different picture, in agreement with two earlier studies [12, 13]. As demonstrated in detail in [10], the air-water system corresponds to an inner “fluid” of vanishing inertia, surrounded by an ideal fluid.

Firstly, the scaling exponent  $\alpha$  was found to be close to  $1/2$ , (typical values reported in the literature are  $0.56$  [9] and  $0.57$  [10]), which means that breakup is much faster than in the fluid-fluid case, and surface tension must become irrelevant as a driving force. Secondly, the value of  $\alpha$  appeared to depend subtly on the initial condition [11], and was typically found to be larger than  $1/2$ . This raised the possibility of an “anomalous” exponent, selected by a mechanism as yet unknown. To illustrate the qualitative appearance of the pinch-off of a bubble, in Fig. 1 we show a temporal sequence of profiles, using a full numerical simulation of the inviscid flow equations [5]. We confine ourselves to axisymmetric flow, which experimentally is found to be preserved down to a scale of a micron [10], provided the experiment is aligned carefully [9].

The only existing theoretical prediction [7, 11, 15] is based on treating the bubble as a (slightly perturbed) cylinder [12, 13]. This leads to the exponent being  $1/2$  with logarithmic corrections, a result which harks back to the 1940’s [16]. Our numerics, to be reported below, are inconsistent with this result. Moreover, a cylinder is not a particularly good description of the actual profiles (cf.

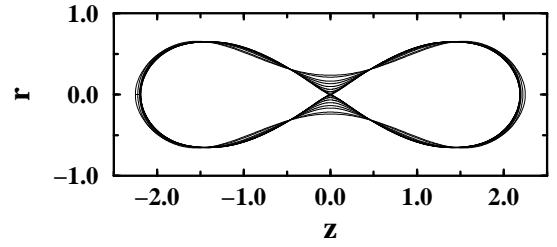


FIG. 1: Numerical simulation of the time evolution of bubble pinch-off from initial conditions given by the shape with the largest waist. Pinch-off is initiated by surface tension, but the late stages are dominated by inertia, as observed experimentally [10].

Fig. 1), as has been remarked before [9]. In this Letter, we present a systematic expansion in the slenderness of the cavity, which is found to lead to a self-consistent description of pinch-off. Our results are in excellent agreement with numerical simulations, and consistent with the experimentally observed exponents.

Our approach is based on the standard description [17, 18] of slender cavities, an assumption that is tested self-consistently by showing that the cavity’s axial extension is greater than its radius. The inviscid, irrotational, incompressible flow  $\mathbf{u} = \nabla\phi$  outside the cavity of length  $2L$  is written as

$$\phi = \int_{-L}^L \frac{C(\xi)d\xi}{\sqrt{(z-\xi)^2 + r^2}}, \quad (1)$$

where  $C(\xi)$  is a line distribution of sources to be determined. The length  $L$  will later drop out of the description of the pinch region, as indeed (1) is not expected to be good near the ends of the bubble. For a slender geometry,  $\partial_z\phi \ll \partial_r\phi$ , and the radial velocity, again using slenderness, is easily evaluated to be  $\partial_r\phi = -2C(z)/h(z)$ .

The equation of motion for the collapsing cavity of radius  $h(z, t)$  is  $\partial_t h \approx u_r$ , and thus  $\dot{a}(z, t) \approx -4C$ , where  $a = h^2$  and the dot denotes the time derivative. Finally, an equation of motion for  $C$  comes from the Bernoulli

equation, evaluated at the free surface [19]. We then arrive at

$$\int_{-L}^L \frac{\ddot{a}(\xi, t) d\xi}{\sqrt{(z - \xi)^2 + a(z, t)}} = \frac{\dot{a}^2}{2a} + 4\Delta p/\rho, \quad (2)$$

where  $\Delta p = \gamma\kappa + \text{const}$  is the pressure difference across the cavity [20]. In the two-fluid problem, the surface tension  $\gamma$ , multiplied by the mean curvature  $\kappa \approx 1/h$ , drives the problem. The capillary pressure will however turn out to be subdominant, so the last term in (2) can effectively be neglected. Note that the resulting equation is invariant under a rescaling of both space and time, as both remaining terms are inertial (describing acceleration and convection of a fluid element). Thus dimensional arguments do not work, and a more detailed analysis is needed to fix the scaling exponent. Note that (2) does not conserve the volume of the cavity, whereas Fig. 1 assumes an incompressible gas inside the bubble. This however only affects the rounded ends of the bubble.

Our aim is to explain the observed scaling behavior of the minimum cross section  $a_0 = a(0, t)$ , as well as of the axial length scale  $\Delta$  of the profile, which can be characterized by the inverse curvature  $\Delta \equiv (2a_0/a_0'')^{1/2}$ , where  $a_0'' = a''(0, t)$  and the prime denotes a derivative with respect to  $z$ . Experiments as well as our own simulations show that  $a_0 \approx At'^{2\alpha}$  and  $\Delta \approx Dt'^\beta$  with  $\beta < \alpha$ , thus the radius is small compared to the axial extend at the minimum. This means that  $a(0, t)$  can be neglected relative to  $\xi^2 \approx \Delta^2$  in the denominator of the integral, except near the position  $\xi = 0$  of the minimum. In other words, the integral is dominated by *local* contributions near the minimum. This will permit us to find equations of motion for the minimum in terms of local quantities alone.

As shown later,  $\ddot{a}(\xi, t)$  goes to zero over the axial scale  $\Delta$ . Thus the integral at  $z = 0$  can be approximated as

$$\ddot{a}_0 \int_{-\Delta}^{\Delta} [\xi^2 + a_0]^{-1/2} d\xi \approx \ddot{a}_0 \ln(2\Delta^2/a_0).$$

An arbitrary factor inside the logarithm depends on the exact shape of  $\ddot{a}(\xi, t)$ ; it can be determined empirically, but in fact becomes subdominant in the limit  $a_0'' \rightarrow 0$ . However, we now need another equation for the (time-dependent) width  $\Delta$  to close the description. To that end we evaluate the second derivative of (2) at  $z = 0$ .

The contribution of the left hand side of (2) is

$$\int_{-\Delta}^{\Delta} \ddot{a}(\xi, t) \left[ \frac{2\xi^2 - a_0}{\sqrt{\xi^2 + a_0}^5} - \frac{a_0''}{2\sqrt{\xi^2 + a_0}^3} \right] d\xi.$$

For a slender profile,  $a_0''$  is subdominant, but the integral over the first term in angular brackets conspires to give zero in the limit  $a_0 \rightarrow 0$ , so the second term has to be considered as well, and  $\ddot{a}(\xi, t)$  has to be expanded beyond the constant term:  $\ddot{a}(\xi, t) = \ddot{a}_0 + \ddot{a}_0''\xi^2/2$ . Thus using the same reasoning as before, and keeping in mind that

$a_0' = 0$ , we find for the second derivative of the integral

$$\int_{-\Delta}^{\Delta} \left[ \frac{(\ddot{a}_0 + \ddot{a}_0''\xi^2/2)(2\xi^2 - a_0)}{\sqrt{\xi^2 + a_0}^5} - \frac{\ddot{a}_0 a_0''}{2\sqrt{\xi^2 + a_0}^3} \right] d\xi \approx \left[ \ddot{a}_0'' \ln \left( \frac{4\Delta^2}{e^3 a_0} \right) - 2 \frac{\ddot{a}_0 a_0''}{a_0} \right].$$

Equating this with the second derivative of the right hand side of (2),  $(\dot{a}^2/(2a))''$ , which is readily computed in terms of  $a_0$  and  $\Delta$ , yields the desired second equation. It is slightly more convenient to rewrite the results as equations for the time-dependent exponents

$$2\alpha \equiv -\partial_\tau a_0/a_0, \quad 2\delta \equiv -\partial_\tau a_0''/a_0'', \quad (3)$$

where  $\tau \equiv -\ln t'$  and  $\beta = \alpha - \delta$ . Note that (3) is going to be the “true” definition of the (time-dependent) exponents, which agrees with a local power-law fit. The result is

$$\begin{aligned} (\alpha_\tau + \alpha - 2\alpha^2) \ln(\Gamma_1/a_0'') &= -\alpha^2, \\ (\delta_\tau + \delta - 2\delta^2) \ln(\Gamma_2/a_0'') &= 2\alpha - 3\alpha^2 - 2\alpha\delta + 2\alpha_\tau, \end{aligned} \quad (4)$$

where the subscript denotes the  $\tau$ -derivative.

The scaling factors  $\Gamma_1, \Gamma_2$  have to be determined empirically, but only make a subdominant contribution as  $a_0''$  goes to zero. The time dependence of  $a_0''$  is best found from integrating

$$\ln(a_0'')_\tau = -2\delta. \quad (6)$$

An analysis of (4)-(6) shows that the approach to the singularity corresponds to an *unstable* fixed point as  $\tau \rightarrow \infty$ . As usual, this is the result of the freedom in the choice of singularity time  $t_0$ , see for example [5]. The limit  $\alpha = 1/2$  thus has to be imposed onto the system in order to find the physically relevant solution. From the first equation, one finds that  $\alpha$  approaches 1/2 from above, while the second equation says that  $\delta$  goes to zero, but remains positive. This guarantees the self-consistency of our approximation, although  $\beta$  approaches  $\alpha$  in the limit. However, the approach of  $\alpha$  and  $\beta$  toward their limiting values is exceedingly slow, as seen from the expansion

$$\alpha = 1/2 + \frac{1}{4\sqrt{\tau}} + \frac{\Gamma}{\tau}, \quad \delta = \frac{1}{4\sqrt{\tau}} + O(\tau^{-3/2}), \quad (7)$$

where  $\Gamma$  is a constant which reflects the arbitrariness of the timescale in (2). Thus the value of  $\Gamma$  necessarily depends on initial conditions. However to leading order  $\alpha$  approaches its limiting value in a universal fashion. Finally, for the self-consistency of our analysis we need that the dimensionless parameter  $a_0''$  goes to zero toward pinch-off, as is indeed found from (6), owing to the slowness with which  $\delta$  converges toward zero.

We now turn to a detailed comparison with full numerical simulations, not relying on any slenderness assumption, by focusing on the late stages of the pinch-off

event shown in Fig. 1. To this end a suitably modified version of the boundary integral code developed to examine inviscid droplet pinch-off [5] was used, as originally reported in [14]. This involved two important modifications: First, the boundary value operator (cf. Equation (11) in [5]) has a zero eigenvalue in the case of the absence of an inner fluid, corresponding to a change in the bubble volume. This singularity is analytically removed before the boundary integral operator is inverted, fixing the bubble volume. Second, due to the rapidity of bubble pinch-off, the adaptive time-stepping used for droplet pinch-off in [5] was replaced by a time-step halving procedure with error estimation.

A comparison of the numerical simulations with (7) is given in Fig. 2. Using equation (3), the value of  $\alpha$  from the numerical simulations can be calculated as  $\alpha = t' \partial_{t'} h_0 / h_0$ , and the pinch-off time  $t_0$  is estimated from the numerical data. The solid curve in Fig. 2 is the data from the numerical simulation, the dashed curve is the leading order prediction given by equation (7) with  $\Gamma = 0$ , and the dotted curve includes the adjustable constant with  $\Gamma = 0.1$ .

Data from the numerical simulations can be divided into three regimes. From approximately  $10^{-12} < t' < 10^{-4}$  the bubble is considered to be in the asymptotic regime, and it is seen that there is very good agreement between the numerical data and the asymptotic theory: the leading order theory with  $\Gamma = 0$  accurately predicts the extremely slow decrease in the numerically determined value of  $\alpha$ , and the second order correction with  $\Gamma = 0.1$  improves the agreement between the asymptotic theory and the numerical data. Equally good agreement was found for numerical runs using other initial conditions, provided that  $\Gamma$  was adjusted, as it is expected to depend on initial conditions, as also observed in experiment [11]. Time  $t' > 10^{-4}$  corresponds to a transitional regime where the bubble adjusts from an initial state where surface tension is required to initiate pinch-off, to an asymptotic state where surface tension is irrelevant. Time  $t' \sim 10^{-12}$  represents the threshold of the numerical simulations: extremely large interfacial velocities acting over ever-decreasing lengthscales, ultimately puts a limit on the validity of the numerical simulations.

Gordillo et al. [7, 15] have previously predicted that the minimum bubble radius  $h_0$  should scale with  $t'$  according to  $t' \propto h_0^2 \sqrt{-\ln h_0^2}$ , using a method that in many respects is similar to ours [15]. However, the crucial difference is that they do not treat the axial length scale  $\Delta$  as a dynamical variable as we do, but effectively identify  $\Delta$  with some outer length scale. Indeed, if one replaces  $a_0''$  by  $a_0$  in (4), one recovers the scaling result of [15]. The conceptual difference between the two approaches is illustrated further by Fig. 3, which shows the central peak of  $\ddot{a}$  from the full numerical simulation. The value of  $\ddot{a}$  rapidly drops to zero, effectively providing the cutoff of the integral (2) at an axial length  $\Delta$ , which is shrinking like  $t'^\beta$ . So far, we have not been able to identify the logarithmic corrections of  $\beta$  in our full numerical sim-

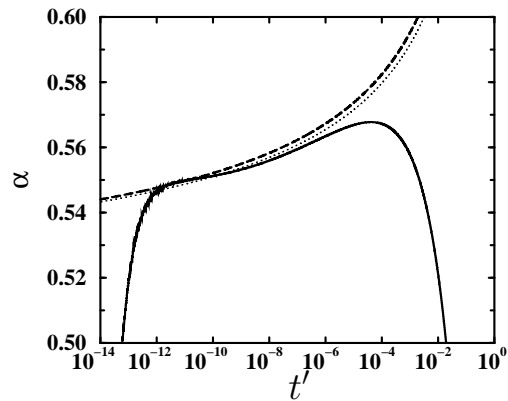


FIG. 2: A comparison of the exponent  $\alpha$  between full numerical simulations of bubble pinch-off (solid line) and the leading order asymptotic theory with  $\Gamma = 0$  (dashed line) and the second order correction with  $\Gamma = 0.1$  (dotted line).

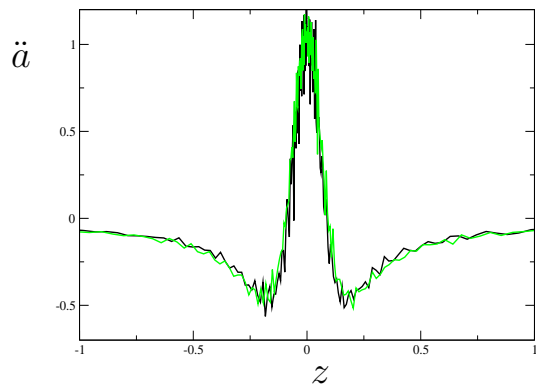


FIG. 3: A normalized graph of  $\ddot{a} = \partial^2 h^2(z, t) / \partial t^2$  as given by the full numerical simulations, for two different initial conditions, and at  $t' = 3.8 \times 10^{-10}$  (black line) and  $t' = 2.1 \times 10^{-10}$  (green line).

ulations, since computing the axial scale is much more demanding than computing  $h_0$ .

In Fig. 4 we plotted the numerically computed minimum radius  $h_0$ , divided by the universal part of the present theory (full line), and that of [15] (dashed line). If normalized by an appropriate constant, the result should be unity. Namely, (7) with  $\Gamma = 0$  is equivalent to  $h_{0,pred} \propto t'^{1/2} \sqrt{e^{-\sqrt{-\ln t'}}}$ , while the theory in [7] amounts to  $h_{0,pred} \propto t'^{1/2} / (-\ln h_0^2)^{1/4}$ . While the present theory agrees extremely well with numerics without the use of any adjustable constant, the theory in [15] varies by approximately  $\pm 50\%$  over the range of  $t'$  plotted.

In our earlier numerical simulations [14], as well as in most experimental papers [6, 9, 10], the data for the minimum radius was represented by adjusting a single exponent  $\bar{\alpha}$ . Although Fig. 2 clearly shows that the exponent is slowly varying, this subtle feature is difficult to detect in a more conventional plot like Fig. 4. To

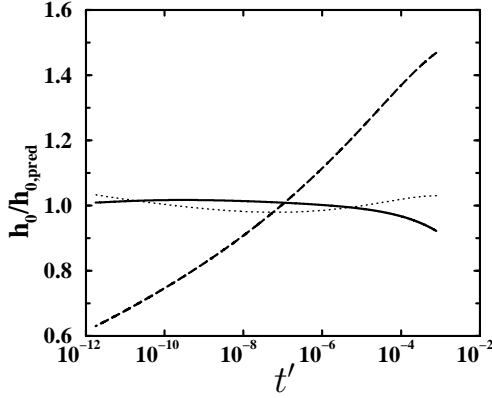


FIG. 4: A normalized graph of  $h_0/h_{0,pred}$  where  $h_{0,pred}$  is predicted according to the theory presented by Gordillo et al. [7] (dashed line), a least square approximation [14] (dotted line), and the current asymptotic theory with  $\alpha = 1/2 + \frac{1}{4\sqrt{\tau}}$  (solid line).

demonstrate this point, we have determined an effective exponent  $\bar{\alpha} = 0.559$  from a least-square fit to the numerical data, a value which is close to those observed experimentally [9, 10]. In essence,  $\bar{\alpha}$  can be viewed as the average over  $\alpha$  values shown in Fig. 2. The resulting fit (dotted line) gives a surprisingly good description of

the data, as a result of the extremely slow variation of  $\alpha$ . It also highlights the need for more sophisticated plots like Fig. 2 in the interpretation of future (experimental) data.

To summarize, we have developed an asymptotic theory for the collapse of an axisymmetric cavity. A novel feature of this theory is a slow variation of the scaling exponents, whose leading order contributions are universal. The slowness of the approach explains the experimental observation of apparently new scaling exponents, whose value may depend weakly on initial conditions. It remains to calculate the entire form of the central peak of  $\ddot{a}$ , which according to Fig. 3 is universal. This will determine the values of the constants  $\Gamma_1$  and  $\Gamma_2$ . Other challenges are the inclusion of non-axisymmetry [9] and viscosity [10] into the theoretical description.

### Acknowledgments

We thank J. Lister for his continued support, valuable insight, and very detailed comments on the manuscript, as well as J.M. Gordillo for discussions. S. Thoroddsen made his experiments available to us prior to publication, for which we are grateful. JHS acknowledges financial support from a Marie Curie European Fellowship FP6 (MEIF-CT2006-025104).

- 
- [1] J. Eggers, *Rev. Mod. Phys.* **69**, 865 (1997).
  - [2] J. Eggers, *ZAMM* **85**, 400 (2005).
  - [3] Y.J. Chen and P.H. Steen, *J. Fluid Mech.* **341**, 245-267 (1997).
  - [4] R. F. Day, E. J. Hinch, and J. R. Lister, *Phys. Rev. Lett.* **80**, 704 (1998).
  - [5] D. Leppinen and J.R. Lister, *Phys. Fluids* **15**, 568 (2003).
  - [6] J.C. Burton, R. Waldrep, and P. Taborek, *Phys. Rev. Lett.* **94**, 184502 (2005).
  - [7] J.M. Gordillo et al., *Phys. Rev. Lett.* **95**, 194501 (2005).
  - [8] S.T. Thoroddsen, E.G. Etoh, and K. Takeara, *Bull. Am. Phys. Soc.* **50**, BD.00002 (2005).
  - [9] N.C. Keim et al., *Phys. Rev. Lett.* **97**, 144503 (2006).
  - [10] S.T. Thoroddsen, E.G. Etoh, and K. Takeara, submitted to *Phys. Fluids* (2006).
  - [11] R. Bergmann et al., *Phys. Rev. Lett.* **96**, 154505 (2006).
  - [12] M.S. Longuet-Higgins, B.R. Kerman, and K. Lunde, *J. Fluid Mech.* **230**, 365 (1991).
  - [13] H.N. Ögüz and A. Prosperetti, *J. Fluid Mech.* **257**, 111 (1993).
  - [14] D. Leppinen, J.R. Lister, and J. Eggers, *Bull. Am. Phys. Soc.* **50**, BD.00006 (2005).
  - [15] J.M. Gordillo and M. Pérez-Saborid, *J. Fluid Mech.* **562**, 303 (2006).
  - [16] N. Levinson, *Ann. Math.* **46**, 704 (1946).
  - [17] H. Ashley and M. Landahl, *Aerodynamics of Wings and Bodies*, Addison-Wesley, Reading, Mass. (1965).
  - [18] V.V. Serebryakov, Proceedings of the International Summer Scientific School, "High Speed Hydrodynamics", Chebocary (2002).
  - [19] L. D. Landau and E. M. Lifshitz, *Fluid Mechanics* Pergamon, Oxford (1984).
  - [20] Equation (2), as it stands, is however ill-posed. Namely, if  $a(z, t)$  in the denominator of the integral operator is assumed constant, the operator can be inverted by Fourier transform. One finds that the high-wavenumber modes of  $\ddot{a}$  grow like  $\exp(k\sqrt{a})$ , so the evolution (2) will soon be polluted by short-wavelength noise. However, this problem can be dealt with completely by adding a small "damping" term  $\epsilon \ddot{a}'' a$  to the right hand side. Choosing  $\epsilon = 10^{-3}$ , we find that the evolution is completely stable, yet the damping term and its derivatives is always uniformly smaller than the other terms by more than 4 orders of magnitude.